

Cloud Optical Depth Retrieval via Sky's Infrared Image For Solar Radiation Prediction

Open
Access

Lai Kok Yee¹, Tan Lit Ken^{1,2,*}, Yutaka Asako¹, Lee Kee Quen¹, Chuan Zun Liang³, Wan Nur Syahidah³, Koji Homma⁴, Gerald Pacaba Arada⁵, Gan Yee Siang⁶, Tey Wah Yen¹, Calvin Kong Leng Sing¹, Jane Oktavia Kamadinata¹, Akira Taguchi²

- ¹ Malaysia – Japan International Institute of Technology (MJIIT), Universiti Teknologi Malaysia Kuala Lumpur, Jalan Sultan Yahya Petra (Jalan Semarak), 54100 Kuala Lumpur, Malaysia
- ² Department of Computer Science, Faculty of Knowledge Engineering, Tokyo City University, 1-28-1, Tamazutsumi, Setagaya-ku, Tokyo, 158-8557, Japan
- ³ Faculty of Industrial Sciences & Technology, Universiti Malaysia Pahang, Lebuhraya Tun Razak, 26300 Gambang, Pahang, Malaysia
- ⁴ International Center, Tokyo City University, 1-28-1, Tamazutsumi, Setagaya-ku, Tokyo, 158-8557, Japan
- ⁵ Electronics and Communications Engineering Department, Gokongwei College of Engineering, De La Salle University, Taft Avenue, Manila, Philippines
- ⁶ Research Center for Healthcare Industry Innovation, National Taipei University of Nursing and Health Sciences, Taipei, Taiwan

ARTICLE INFO

ABSTRACT

Article history:

Received 2 November 2018
Received in revised form 8 May 2019
Accepted 23 May 2019
Available online 6 June 2019

Photovoltaic (PV) system is developed to harness solar energy as an alternative energy to reduce the dependency on fossil fuel energy. However, the output of the PV system is not stable due to the fluctuation of solar radiation. Hence, solar radiation prediction in advanced is needed to make sure the tap changer in PV system has enough time to respond. In this research, the cloud base temperature is identified from the sky's thermal image. From the cloud base temperature, cloud optical depth (COD) is calculated. Artificial neural network (ANN) models are established by using different combinations of current solar radiation and COD to predict the solar radiation several minutes in advanced. R-squared value is used to measure the accuracy of the models. For prediction in advanced for every minute, with COD as input, always show the highest R-squared value. The highest R-squared value is 0.8899 for the prediction for 1 minute in advanced and dropped to 0.5415 as the minute of prediction in advanced increase to 5. This shows that the proposed methodology is suitable for prediction of solar radiation for short term in advanced.

Keywords:

cloud optical depth; infrared image; solar radiation prediction; artificial neural network

Copyright © 2019 PENERBIT AKADEMIA BARU - All rights reserved

1. Introduction

Over the past ten years, due to global warming, the average temperature of the Earth has risen order to reduce the emission of greenhouse gases from fossil fuel energy, alternative energy such as renewable energy is needed to replace fossil fuel energy. There are many types of renewable energy

* Corresponding author.

E-mail address: tlken@utm.my (Tan Lit Ken)

such as solar energy, wind energy, and biomass energy. However, not all renewable energy is suitable to be used as alternative energy because some of them will cause pollution and damage to the environment [1, 2]. So, among all renewable energy, solar energy has proven to be an effective alternative and clean source, abundant and everlasting source of renewable energy [3-5]. The annual average value of solar radiation is thus taken as the solar constant (I_{sc}) which equals to 1367 W/m^2 [6]. However, not all the solar radiation will reach on the surface of Earth. This is due to the albedo of Earth's surface and clouds reflecting the solar radiation back into space[7]. The solar radiation measured on the Earth's surface fluctuates all the day. Figure 1 shows the measured solar radiation throughout a day.

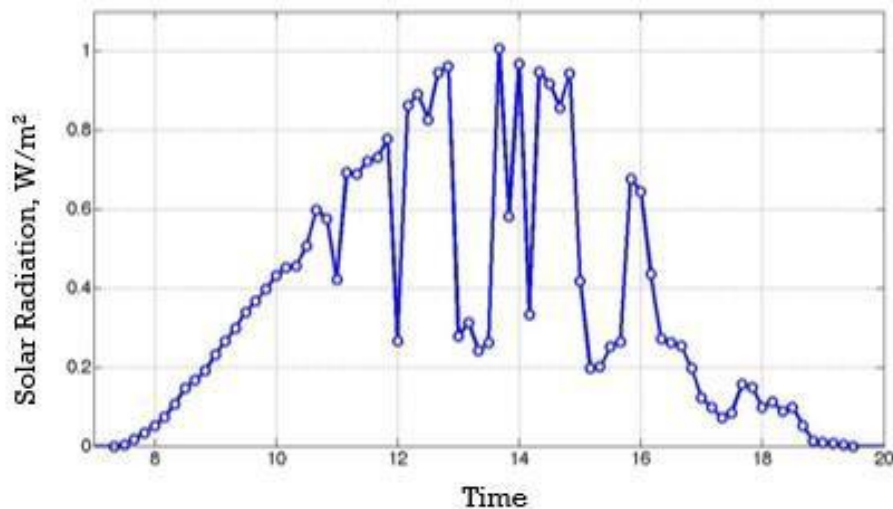


Fig. 1. Measured solar radiation during daytime

Among all solar harnessing technologies, photovoltaic (PV) system is commonly used in household and industry [8]. PV devices can generate electricity directly from the sunlight due to the electronic process that occurs in the built material which is a semiconductor. The output of PV devices depends on the number of solar radiation strikes on the PV devices. Due to the fluctuations of solar energy throughout the day caused by meteorological conditions, the output power of PV devices also fluctuates. The automated line equipment on distribution feeders will be triggered due to the voltage fluctuations and leads to an increase in huge maintenance costs for utilities. Therefore, a constant load is given to counteract the fluctuations. However, this would require a secondary power source such as energy storage that could ramp up or ramp down at high frequencies to provide the load needed. Therefore, solar radiation prediction in advanced is needed for the energy storage reacts few minutes in advance before the fluctuation of solar radiation to ensure the stability of the output of PV system [9, 10].

By using satellite observing systems, the solar radiation fluxes in and out of the climate system at the top of atmosphere are now can be determined [11]. With this, an accurate estimation of the impact of clouds on the top of atmosphere radiation budget can be determined through the comparison of satellite measurements representing all-sky and clear-sky conditions [12]. The Earth's energy budget shows the balance between incoming solar energy from the Sun and outgoing radiation from the Earth [13]. According to Earth's energy budget in Figure 2, solar radiation reaching the surface of the Earth is affected by three factors which are atmosphere, clouds and Earth's surface. In overall, clouds reflected 20% incoming solar radiation and absorbed 3% of it before the solar radiation reaches Earth's surface. While for atmosphere, it reflects 6% of incoming solar radiation and absorbs 16% of it. From this, clouds are identified as the main factors affecting the incoming solar

radiation. According to [14], clouds were also the largest uncertainty in the Global Climate Models (GCMs).

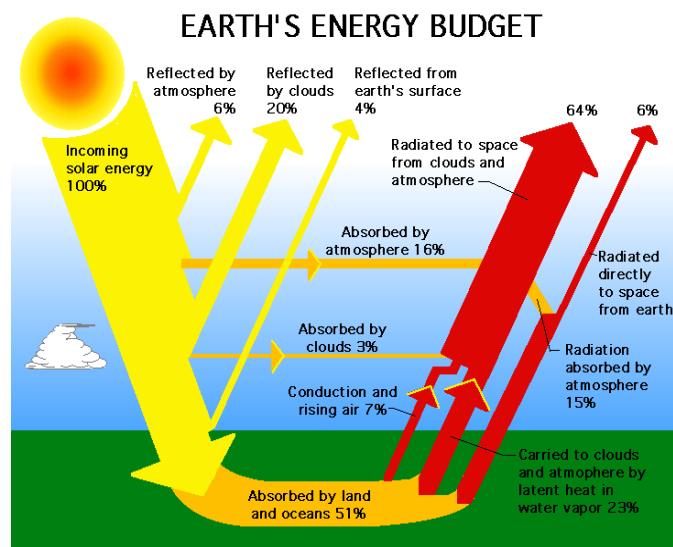


Fig. 2. Earth's Energy Budget [13]

Cloud optical depth (COD), a dimensionless magnitude, is an attenuation measure of the solar radiation through the cloud due to scattering and absorption by cloud's particles [15]. The COD depends on its physical constitution, the form, the concentration of the particles and the vertical thickness of the cloud. This is due to thicker clouds consists of more particles to absorb or scatter the incoming solar energy. There are many methodologies have been carried out to obtain the COD data. However, most of them require a lot of equipment. For example, in the methodology proposed by Serrano in 2014 [16], sky camera and radiometer are used to obtain COD data. While in 2017, Marin [17] obtained COD data by using several types of equipment which are radiometer, pyranometer, sunphotometer, ceilometer, and Ozone Monitoring Instrument (OMI). Thus, this increases the complexity and cost in order to obtain COD data.

For the prediction part, many researchers used different meteorological data and geographical data as input to predict solar radiation. ANN models have been established to predict the solar radiation because the conventional or empirical models are less accurate [18-21]. However, those researches involve a lot of information to establish the ANN models. For example, some of them use geometrical data like longitude, latitude, and altitude for the establishment of data [22-24]. While some of them use meteorological data such as duration of sunshine, temperature and relative humidity for prediction [24-26]. The high number of input increases the cost of equipment and computational time of ANN models.

In this paper, a new methodology to obtain COD data based on the cloud base temperature is proposed. Then, the obtained COD data with solar radiation are used to predict solar radiation in advanced. ANN is used for the prediction due to its ability in achieving fast and accurate prediction. Unlike existing methodologies, the proposed methodology only requires COD data and solar radiation data. This will reduce the complexity of obtaining all meteorological data and cost in preparing equipment.

2. Methodology

In this research, a ground-based infrared camera is used to capture the thermal image of the sky at 30 seconds interval of time in this research. In this chapter consists of 4 sections which are data collection from infrared sky images, calculation of radiation absorbed by clouds, calculation of cloud optical depth and establishment of ANN model. Figure 3 shows the flowchart of the methodology to achieve COD from sky thermal image.

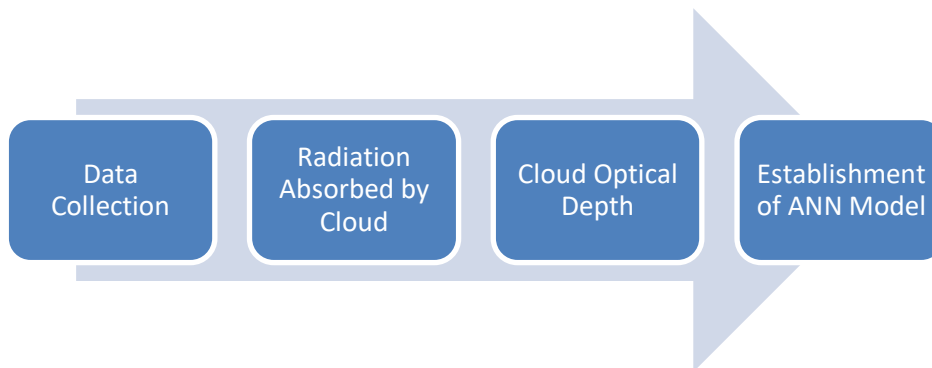


Fig. 3. Flowchart of research methodology

2.1 Data Collection

This research focuses only on the clouds that moving toward the Sun. This is due to cloud movement towards the Sun will greatly affect the irradiance. The purpose of this is to record the changes in cloud thermal distribution and cloud coverage with respect to time. One line and three lines will be drawn across the same images separately and cloud base temperature along the lines will be identified. Figure 4 and Figure 5 show the reference line where the pixels along the line will be analyzed to obtain the cloud base temperature.

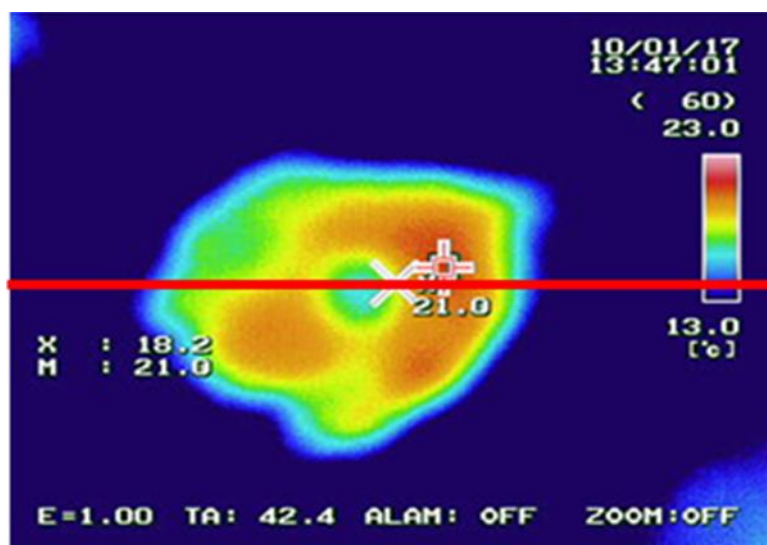


Fig. 4. One reference line is drawn on the sky thermal image

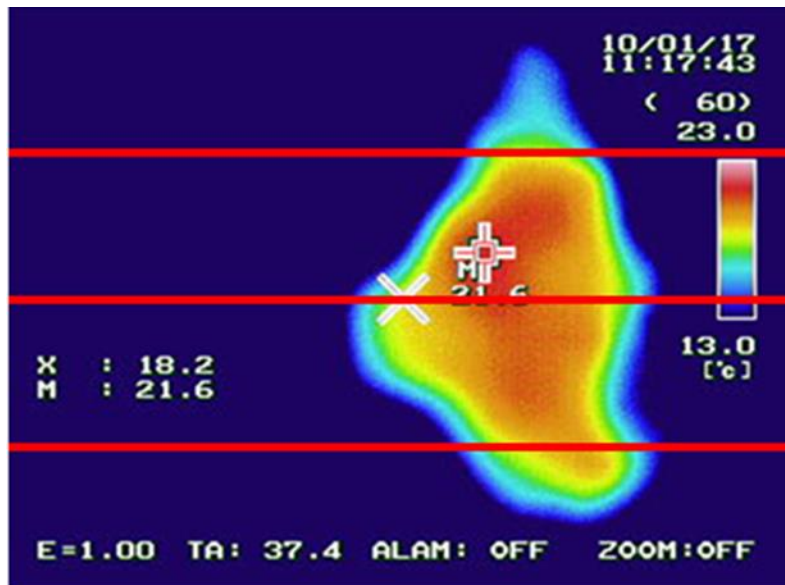


Fig. 5. Three reference lines are drawn on the sky thermal image

Each line only has 380 pixels that will undergo the extraction of RGB information process. To make sure that the image can clearly show the temperature distributions of the sky and cloud, the temperature range setting of the infrared camera is set from 13°C to 23°C as shown in Figure 3. This is because the average cloud base temperature is around 18°C.

2.2 RGB to Temperature Conversion

The true colour value obtained is then converted into the temperature using the following equation.

$$T = \frac{TCV}{16777216} * T_R + T_{min} \quad (1)$$

where T is the temperature of each pixel, T_R is temperature range=10 and T_{min} is minimum temperature= 13°C.

To shorten the computational time, only the true colour value in the middle of the image will be undergoing the conversion. Since the range of temperature is from 13°C to 23°C, the temperature of each pixel is calculated based on the ratio of the true colour value obtained and the total true colour value. This is because the temperature setting of the infrared camera is set within this 10°C.

2.3 Radiation Absorbed by Cloud

Based on the temperature obtained, radiation absorbed by the cloud is then calculated. Stefan Boltzmann law states that the total radiant energy emitted from a surface is proportional to the fourth power of its absolute temperature. Eq. (2) shows the relationship of radiant energy with temperature.

$$E = \epsilon\sigma T^4 \quad (2)$$

where E is Radiant energy, ϵ is emissivity of cloud, 0.44, and σ is Stefan-Boltzmann constant, $5.67 \times 10^8 \text{ W/m}^2 \text{ K}^4$.

2.4 Transmittance of Cloud

The transmission of cloud (T_C) can be defined as the ratio of downward flux below cloud and downward flux at the top of cloud. Eq. (3) shows the calculation for cloud transmission.

$$T_C = \frac{R_a}{R_b} \quad (3)$$

where R_a is downward flux below cloud and R_b is downward flux at the top of cloud.

2.5 Radiation Flux Above and Below Cloud

To calculate the radiation flux, the information from Earth's energy budget will be used to estimate the radiant flux at the top of cloud. Since the solar radiation reaches the Earth varies from day to day, to calculate the solar radiation reaches on Earth in a specific day, Eq. (4) is used.

$$I_0 = I_{SC} \left[1 + 0.034 \cos \left(2\pi \frac{n}{265.25} \right) \right] \quad (4)$$

where I_0 = Solar radiation reaches the Earth, I_{SC} = Solar constant (1367 W/m^2) and n = the day of the year.

After obtaining the total incoming solar radiation, the solar radiation reaches the top of the cloud is obtained based on the Earth's energy budget. According to Earth's energy budget, 6% of incoming solar radiation is reflected to space by the atmosphere before it reaches the top of the cloud. Therefore, 6% of total incoming solar radiation is deducted from it.

To obtain the radiant flux below the cloud, the remaining 94% of incoming solar radiation is reduced to 74%. This is because 20% of it is reflected to space by cloud according to Earth's energy budget. Then, the remaining 74% of solar radiation is deducted with the solar radiation absorbed by cloud and the results are the radiant flux below the cloud.

2.6 Cloud Optical Depth Retrieval

After obtaining the transmission of cloud, cloud optical depth is calculated using equation below.

$$COD = -\ln T_C \quad (5)$$

2.7 Establishing ANN Model

ANN model is used to predict the solar radiation for 1 - 5 minutes in advanced. For comparison purposes and to show that our proposed approach can improve the accuracy of prediction, a few combinations of data set are used as input to train the models. Four models with different inputs were established for prediction of solar radiation for 1 minute to 5 minutes in advance. The table below shows the examples of inputs and output that were used to train the models for prediction of solar radiation of 1 minute in advanced.

Table 1
 Example of ANN models

No of model	Inputs	Output
1	Current Solar radiation	Solar radiation after 1 minute
2	Current Solar radiation Current COD for one line COD for one line after 30 seconds	Solar radiation after 1 minute
3	Current Solar radiation Current COD for three lines COD for three lines after 30 seconds	Solar radiation after 1 minute
4	Current Solar radiation Change of COD in 30 seconds	Solar radiation after 1 minute

In all ANN models, the data set will be set to divide into three categories. 60% of the data is used for training the model, 20% is for testing and the final 20% is for validation. The purpose of testing is to provide an independent measure of model performance during and after training the data. To measure generalized capability, validation data is used. The Figure 6 illustrates the configuration of the ANN which used in this research.

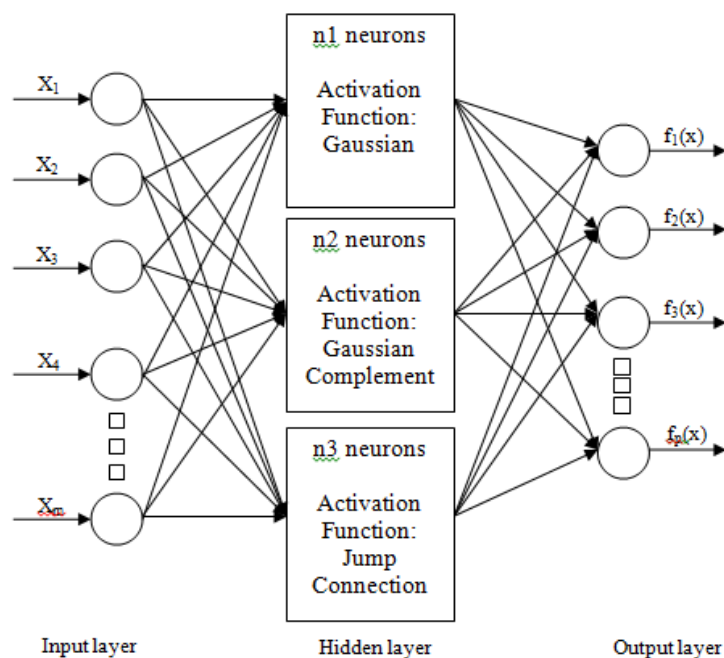


Fig. 6. Artificial neural network configuration

There are three neurons within the hidden layer and each of them has its own activation function. The three activation functions are Gaussian, Gaussian complement and jump connection. The formula of Gaussian activation function is

$$f(x) = e^{-x^2} \tag{6}$$

The formula of Gaussian complement activation function is

$$f(x) = 1 - e^{-x^2} \tag{7}$$

The formula jump connection activation function is

$$f(x) = x \tag{8}$$

In ANN, there are three other parameters that will affect the results which are learning rate, momentum and initial weight. Since the data set of this research is limited, so the network is considered as simple. In this case, the learning rate of the network is set to 0.9. For the rest, momentum and initial weight is set to 0.3 as it gives the most accurate result for all network.

2.8 Performance Evaluation

The performance of the models was evaluated by coefficient of determination (R^2). R-squared or also known as the coefficient of determination is a statistical measure used to show how close the data are fitted to the regression line. The higher the R-squared value indicates a better goodness of fit for the observations.

$$R^2 = 1 - \frac{\sum(y-\hat{y})^2}{\sum(y-\bar{y})^2} \tag{9}$$

where, y = actual value, \hat{y} = predicted value of y and \bar{y} = mean of the y values.

3. Results

3.1 COD for Single Line

Figure 7 shows the sky's infrared image taken on 11.17 am. A red line is drawn in the middle of the image and analysis is carried out on the pixels lay on the line. Figure 8 and Figure 9 are the results of the analysis.

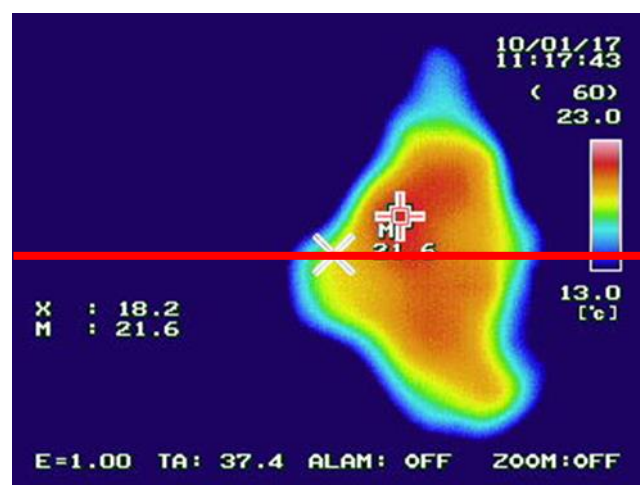


Fig. 7. Sky's thermal image at 11:17:43 a.m

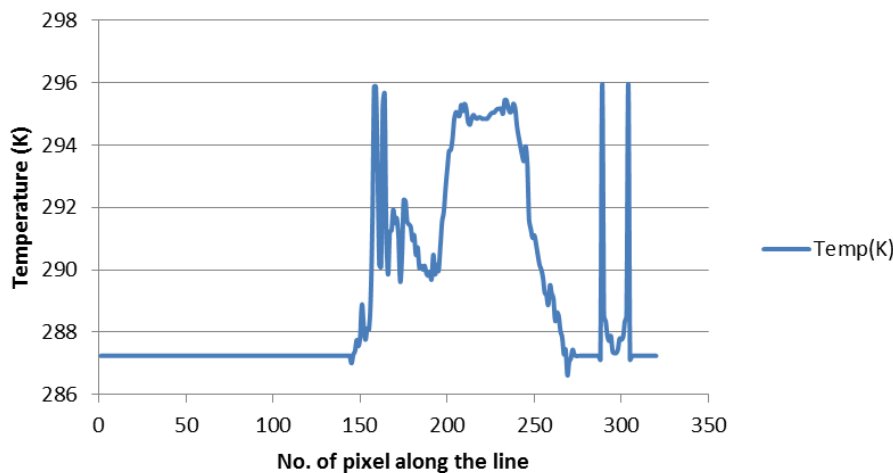


Fig. 8. Temperature graph for Figure 7

By analyzing the pixel along the single red line in Figure 7, COD is obtained from the temperature of the cloud. However, the blue color in the image also indicates a value in term of temperature which is around 14.1°C. This blue color part is identified as clear sky. Hence, all the values that show the same number are eliminated and reset to 0. Figure 8 shows the temperature distribution along the middle horizontal line of Figure 7, while Figure 9 shows the final cloud optical depth value along the horizontal line in the middle of images.

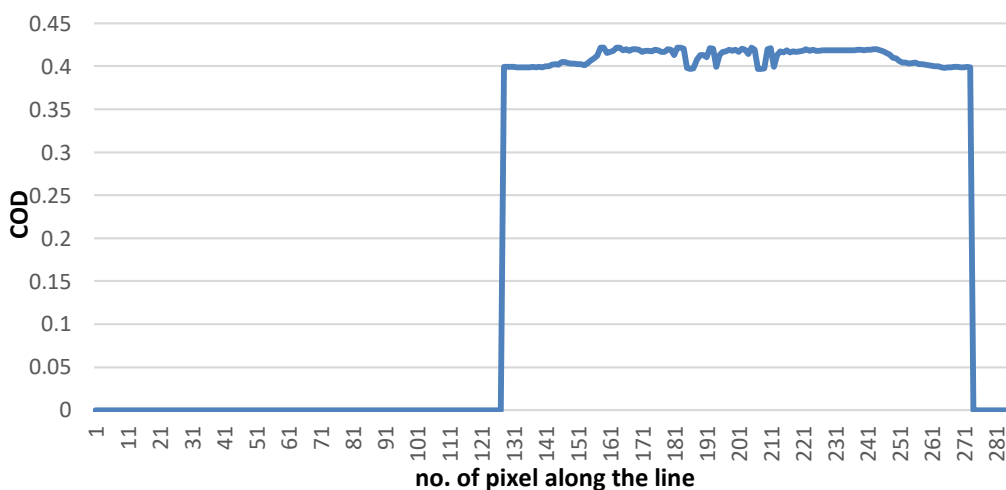


Fig. 9. Cloud optical depth of Figure 7

From Figure 8 and Figure 9, the COD values are proportional to the temperature of the cloud. When the temperature of the cloud is higher, the COD value will also be higher. These results meet the explanation where the thicker the clouds, the absorption and scattering effects by cloud on incoming solar radiation are higher and lead to the high value in COD. Besides that, the COD values of each image show almost the same. This is due to the limitation of the infrared camera which its viewing factor is too small. In order to get the perfect images of the cloud, only small sizes clouds are captured during data collection.

Figure 10 and 11 show the actual solar radiation and the prediction results for solar radiation with COD as input for 1 minute and 5 minutes in advanced. The prediction for 1 minute in advance show high accuracy with $R^2 = 0.8651$, while the mean absolute error is 62.618. For 5 minutes case, the R^2

result dropped to 0.4513 and the mean absolute error is 154.418. From these results, the accuracy of the prediction is going down as the minutes in advanced for prediction of solar radiation increase.

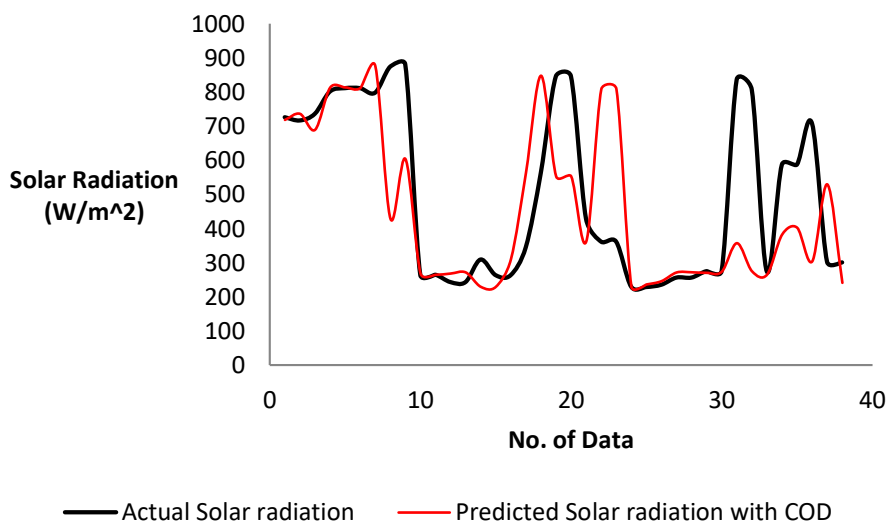


Fig. 10. Actual solar radiation and prediction results for 1 minute in advanced with COD as input

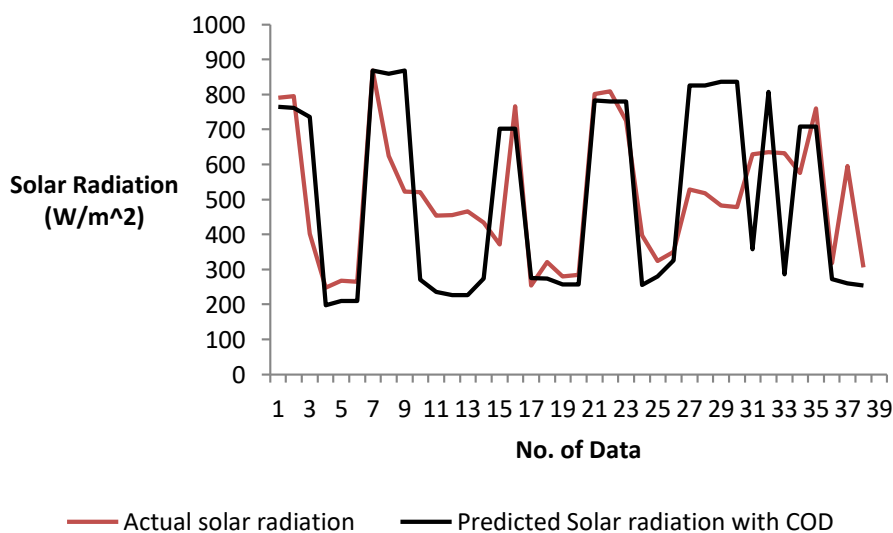


Fig. 11. Actual solar radiation and prediction results for 5 minute in advanced with COD as input

3.2 COD for Three Lines

In this section, three red lines as shown in Figure 12 were analyzed to obtain the COD of the three lines instead of one line. By analyzing the pixel along the three lines, COD is obtained from the temperature of the cloud. The process to obtain the COD of three lines is similar to the process of obtaining COD from single line. The COD of the three lines is then added up together to establish the model for solar radiation prediction. Figures below show the prediction results for 1 minute and 5 minutes in advanced.

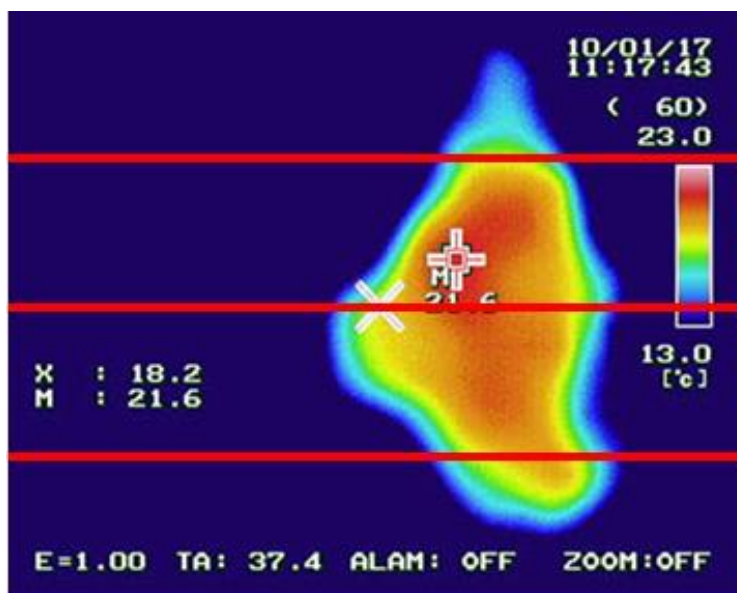


Fig. 12. Sky's thermal image at 11:17:43 a.m

Figure 13 and 14 show the actual solar radiation and the prediction results for solar radiation with COD of three lines as input for 1 minute and 5 minutes in advanced. The prediction for 1 minute in advance show high accuracy with $R^2= 0.8899$, while the mean absolute error is 56.106. For 5 minute case, the R^2 result dropped to 0.5415 and the mean absolute error is 133.4814. From these results, the accuracy of the prediction is going down as the minutes in advanced for prediction of solar radiation increase.

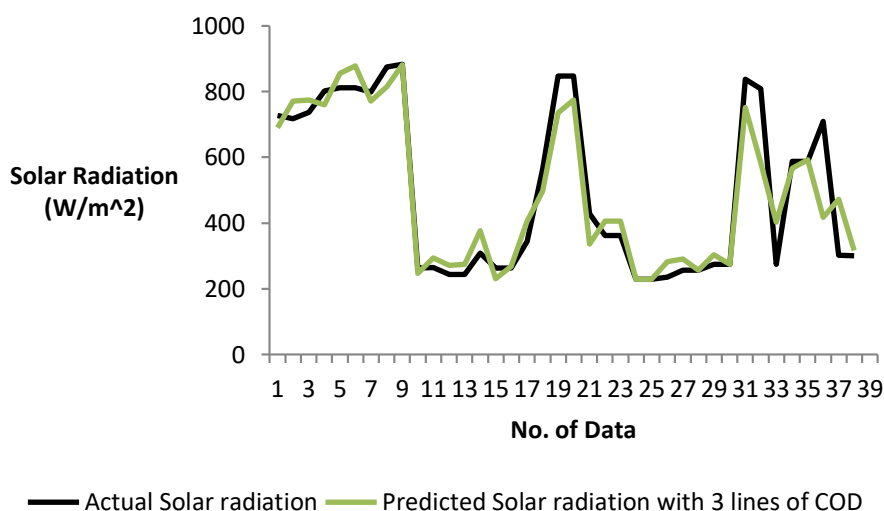


Fig. 13. Actual solar radiation and prediction results for 1 minute in advanced with COD as input

From the graph shown in Figure 15, the results of prediction with COD always show higher than others and biggest difference with the prediction that without COD data as input. When the advanced time for prediction increased, the R-squared values are decreased. Surprisingly, the R-squared results of prediction with COD of single line are almost same with the R-squared results of the prediction with COD of three lines from the images. This means models with COD of single line are enough to establish for solar radiation prediction in advance.

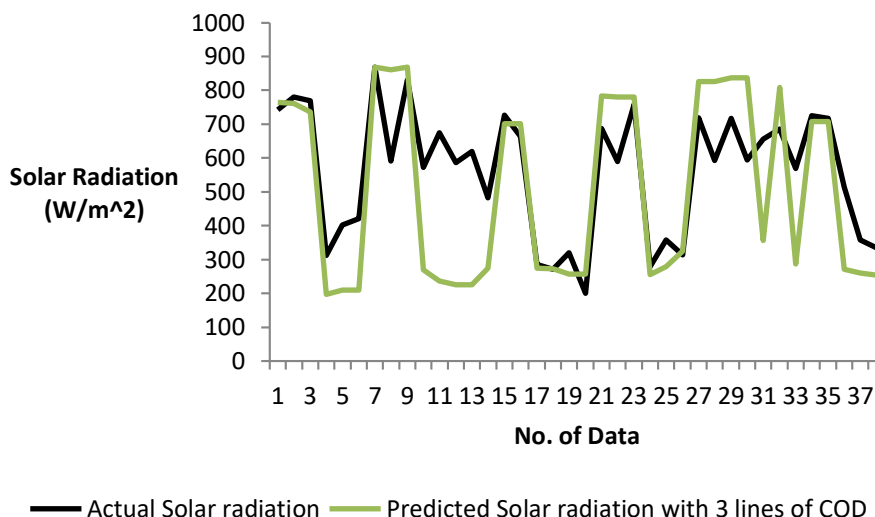


Fig. 14. Actual solar radiation and prediction results for 5 minute in advanced with COD as input

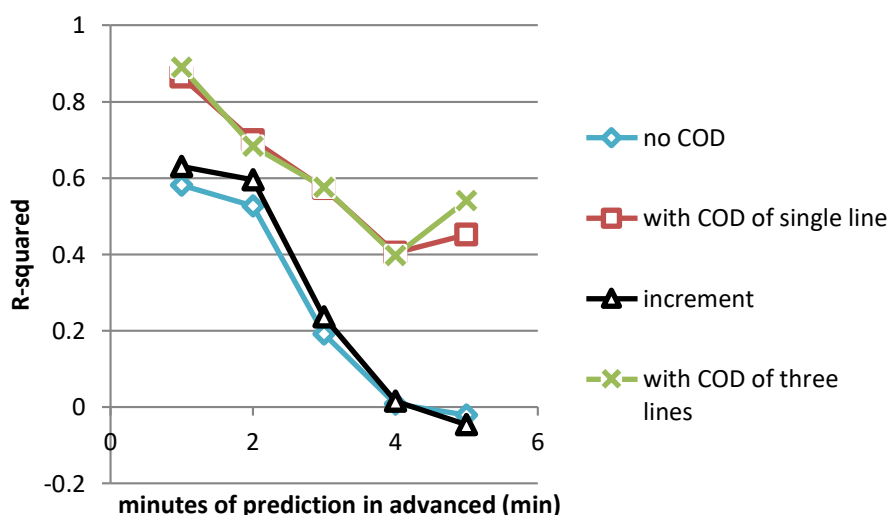


Fig. 15. R-squared results of each prediction

Compare with models with COD increment and models with no COD, a conclusion can be made that the prediction results will be more accurate if COD is used as input and the accuracy is the highest when predicting the solar radiation for 1 minute in advanced.

4. Conclusions

In this paper, we proposed a new methodology to predict the solar radiation in advanced with only cloud optical depth data. We introduced a methodology to obtain cloud optical depth data from the cloud base temperature. We found out that the cloud optical depth is directly proportional to the cloud base temperature. ANN is used for the prediction in this research and capable to achieve high accuracy based on the R2 results. The highest R2 result is 0.8899 for the prediction of solar radiation for 1 minute in advanced with COD of three lines as input. This indicates that the prediction for solar radiation in advanced with only COD data and solar radiation data also can achieve high accuracy.

Acknowledgement

The authors would like to express his appreciation to Universiti Teknologi Malaysia and Takasago Thermal Engineering research grant, Vot No. 4B262 for financial support. This research is also partially supported by the Takasago Thermal Engineering research grant, Vot No. 4B314. The authors would also like to acknowledge Ng Su Ling for the assistance given.

References

- [1] Kikuchi, Ryunosuke. "Adverse impacts of wind power generation on collision behaviour of birds and anti-predator behaviour of squirrels." *Journal for Nature Conservation* 16, no. 1 (2008): 44-55.
- [2] Vezmar, Stanislav, Anton Spajić, Danijel Topić, Damir Šljivac, and Lajos Jozsa. "Positive and negative impacts of renewable energy sources." *International journal of electrical and computer engineering systems* 5, no. 2 (2014): 47-55.
- [3] Sansaniwal, Sunil Kumar, Vashimant Sharma, and Jyotirmay Mathur. "Energy and exergy analyses of various typical solar energy applications: A comprehensive review." *Renewable and Sustainable Energy Reviews* 82 (2018): 1576-1601.
- [4] Abdullah, Amira Lateef, Suhaimi Misha, Noreffendy Tamaldin, and Mohd Afzanizam Mohd. "Numerical Analysis of Solar Hybrid Photovoltaic Thermal Air Collector Simulation by ANSYS." *interactions* 11, no. 2 (2019): 1-11.
- [5] Naamandadin, Nurul Akmal, Chew Jian Ming, and Wan Azani Mustafa. "Relationship between Solar Irradiance and Power Generated by Photovoltaic Panel: Case Study at UniCITI Alam Campus, Padang Besar, Malaysia." *Journal of Advanced Research in Engineering Knowledge* 5, no. 1 (2018): 16-20.
- [6] Johnson, Francis S. "The solar constant." *Journal of Meteorology* 11, no. 6 (1954): 431-439.
- [7] Stocker, Thomas, ed. *Climate change 2013: the physical science basis: Working Group I contribution to the Fifth assessment report of the Intergovernmental Panel on Climate Change*. Cambridge University Press, 2014.
- [8] Abdullah, Ahmed L., S. Misha, N. Tamaldin, M. A. M. Rosli, and F. A. Sachit. "Photovoltaic Thermal/Solar (PVT) Collector (PVT) System Based on Fluid Absorber Design: A Review." *Journal of Advanced Research in Fluid Mechanics and Thermal Sciences* 48, no.2 (2018): 196-208.
- [9] Hirata, Yoshito, Taiji Yamada, Jun Takahashi, Kazuyuki Aihara, and Hideyuki Suzuki. "Online multi-step prediction for wind speeds and solar irradiation: Evaluation of prediction errors." *Renewable energy* 67 (2014): 35-39.
- [10] Huld, Thomas, Richard Müller, and Attilio Gambardella. "A new solar radiation database for estimating PV performance in Europe and Africa." *Solar Energy* 86, no. 6 (2012): 1803-1815.
- [11] Loeb, Norman G., David R. Doelling, Hailan Wang, Wenying Su, Cathy Nguyen, Joseph G. Corbett, Lusheng Liang, Cristian Mitrescu, Fred G. Rose, and Seiji Kato. "Clouds and the earth's radiant energy system (CERES) energy balanced and filled (EBAF) top-of-atmosphere (TOA) edition-4.0 data product." *Journal of Climate* 31, no. 2 (2018): 895-918.
- [12] Wild, Martin, Maria Z. Hakuba, Doris Folini, Patricia Dörig-Ott, Christoph Schär, Seiji Kato, and Charles N. Long. "The cloud-free global energy balance and inferred cloud radiative effects: an assessment based on direct observations and climate models." *Climate dynamics* 52, no. 7-8 (2019): 4787-4812.
- [13] Trenberth, Kevin E., John T. Fasullo, and Jeffrey Kiehl. "Earth's global energy budget." *Bulletin of the American Meteorological Society* 90, no. 3 (2009): 311-324.
- [14] Philander, S.G., *Encyclopedia of Global Warming & Climate Change*. 2012: Thousand Oaks, California.
- [15] Stephens, Graeme L. *Remote sensing of the lower atmosphere*. Vol. 1994. New York: Oxford University Press, 1994.
- [16] Serrano, D., M. Núñez, M. P. Utrillas, M. J. Marín, C. Marcos, and J. A. Martínez-Lozano. "Effective cloud optical depth for overcast conditions determined with a UV radiometers." *International Journal of Climatology* 34, no. 15 (2014): 3939-3952.
- [17] Marín, M. J., D. Serrano, M. P. Utrillas, M. Núñez, and J. A. Martínez-Lozano. "Effective cloud optical depth and enhancement effects for broken liquid water clouds in Valencia (Spain)." *Atmospheric research* 195 (2017): 1-8.
- [18] Khatib, Tamer, Azah Mohamed, and Kamaruzzaman Sopian. "A review of solar energy modeling techniques." *Renewable and Sustainable Energy Reviews* 16, no. 5 (2012): 2864-2869.
- [19] Şenkal, Ozan, and Tuncay Kuleli. "Estimation of solar radiation over Turkey using artificial neural network and satellite data." *Applied Energy* 86, no. 7-8 (2009): 1222-1228.
- [20] Mubiru, J., and E. J. K. B. Banda. "Estimation of monthly average daily global solar irradiation using artificial neural networks." *Solar Energy* 82, no. 2 (2008): 181-187.
- [21] Jiang, Yingni. "Prediction of monthly mean daily diffuse solar radiation using artificial neural networks and comparison with other empirical models." *Energy policy* 36, no. 10 (2008): 3833-3837.

-
- [22] Mohandes, M., S. Rehman, and T. O. Halawani. "Estimation of global solar radiation using artificial neural networks." *Renewable energy* 14, no. 1-4 (1998): 179-184.
 - [23] Jiang, Yingni. "Computation of monthly mean daily global solar radiation in China using artificial neural networks and comparison with other empirical models." *Energy* 34, no. 9 (2009): 1276-1283.
 - [24] Alam, Shah, S. C. Kaushik, and S. N. Garg. "Computation of beam solar radiation at normal incidence using artificial neural network." *Renewable Energy* 31, no. 10 (2006): 1483-1491.
 - [25] Rehman, Shafiqur, and Mohamed Mohandes. "Artificial neural network estimation of global solar radiation using air temperature and relative humidity." *Energy Policy* 36, no. 2 (2008): 571-576.
 - [26] Al-Alawi, S. M., and H. A. Al-Hinai. "An ANN-based approach for predicting global radiation in locations with no direct measurement instrumentation." *Renewable Energy* 14, no. 1-4 (1998): 199-204.